arXiv:1402.4207v1 [cond-mat.mes-hall] 18 Feb 2014

Satellite structures in the spectral functions of semiconductor quantum well two-dimensional electron gases: a GW plus cumulant study

Johannes Lischner, Derek Vigil-Fowler, and Steven G. Louie
Department of Physics, University of California, Berkeley, California 94720, USA, and Materials Sciences Division, Lawrence Berkeley National Laboratory, Berkeley 94720, USA.

We present theoretical calculations for the spectral functions and single-particle densities of states of the two-dimensional electron gas in semiconductor quantum wells at different electron densities using the GW+cumulant method. We compare our results to GW only calculations and find significant differences in the description of the satellites between the two theories: while GW theory predicts the existence of a plasmaron excitation, no such excitation is found in GW+cumulant theory. We compare our results to experimental tunneling spectra from semiconductor quantum wells and find good agreement for the satellite properties.

Introduction.—The two-dimensional electron gas (2DEG) is of fundamental importance to condensed matter physics and has been studied extensively over the past decades. Experimentally, this system can, for example, be realized at a semiconductor heterojunction. Many new phenomena, including the integer [1] and fractional quantum Hall effects [2], were discovered in this system. Recently, there has been much interest in 2DEGs at the interface of oxide materials[3, 4]. Also the theoretical study of the 2DEG has a long history. Due to its conceptual simplicity, this system has served as a test bed for many-body theories of interacting electrons, such as Green's function theories [5, 6] or Quantum Monte Carlo studies[7, 8].

Recently, Dial and coworkers used time-domain capacitance spectroscopy [9, 10] to measure the single-particle density of states (DOS) of a 2DEG with high accuracy [11]. As expected from previous Green's function calculations based on the GW approximation to the electron self energy [5], the experimental DOS of Dial et al. exhibits two features: at low binding energies, a structure due to quasiparticle excitations is observed and, at higher binding energies, a second feature attributed to plasmon satellites is observed as well. However, the onset of the satellite structure in the experiment disagrees with theoretical results from GW theory: GW significantly overestimates the separation between the edges of the quasiparticle and satellite structures.

The failure of GW theory to describe satellites accurately has been found in other systems as well. For the photoemission spectrum of a core state, Langreth [12] demonstrated that the GW theory severely overestimates the quasiparticle-satellite separation and also results in only a *single* satellite instead of a infinite series of satellites. Recently, *ab initio* studies [13–15] reported a similar overestimation of the satellite binding energy for the valence band photoemission spectrum of silicon, and it is found[14] that GW theory does not describe the satellites in angle-resolved photoemission studies of doped graphene [16] accurately.

These studies [12–14] moreover showed that a GW plus cumulant (GW+C) theory [17] which includes significant vertex corrections beyond GW cures the deficiencies of the GW theory for the description of plasmon satellites and gives good agreement with experiments. In particular, while GW predicts a new well-defined excitation in the spectral function, the *plasmaron* [16, 18], resulting from the electron-plasmon coupling, our studies [14] showed for both silicon and doped graphene that no such plasmaron solution exists within the GW+C theory, indicating the spurious nature of the plasmaron.

In this article, we present the first application of the GW+C theory to the 2DEG at a semiconductor heterojunction. Also, for this system, previous calculations based on the GW approximation alone found a plasmaron solution [5, 11]. We present spectral functions and electronic DOSs for different electron densities and compare our results to GW calculations and also to the experimental findings of Dial and coworkers [11]. We do not find a plasmaron solution in the GW+C theory.

Methods.—The current in a tunneling experiment where a voltage difference V is applied across two systems with DOS $g_l(\epsilon)$ and $g_r(\epsilon)$ within the Bardeen formalism is given by[19]

$$I(V) = \int_{\epsilon_F}^{\epsilon_F+eV} d\epsilon g_l(\epsilon) g_r(\epsilon + eV) |M(\epsilon)|^2, \qquad (1)$$

where $M(\epsilon)$ is the tunneling matrix element and ϵ_F and e denote the Fermi energy and the electron charge, respectively. In time-domain capacitance spectroscopy, one system is a three-dimensional electrode and the other a 2DEG. If both the DOS of the three-dimensional electrode and the tunneling matrix element are slowly varying functions of ϵ, the derivative of the current with respect to V is proportional to the DOS of the 2DEG.

The many-body DOS per unit area of a two-dimensional paramagnetic system with a single band, such as an ideal 2DEG, is given by $g(\epsilon) = 2\int d^2k/(2\pi)^2 A_{\boldsymbol{k}}(\epsilon)$ with $A_{\boldsymbol{k}}(\epsilon)$ being the many-body spectral function which is related to the interacting one-

particle Green's function via $A_{\boldsymbol{k}}(\epsilon) = 1/\pi|\mathrm{Im}G_{\boldsymbol{k}}(\epsilon)|$.

Usually, $G_{\boldsymbol{k}}(\epsilon)$ is obtained by solving Dyson's equation $G^{-1}_{\boldsymbol{k}}(\epsilon) = G^{-1}_{0,\boldsymbol{k}}(\epsilon) - \Sigma_{\boldsymbol{k}}(\epsilon) + V^{xc}_{\boldsymbol{k}}$ with $G_{0,\boldsymbol{k}}(\epsilon)$ and $V^{xc}_{\boldsymbol{k}}$ denoting a mean-field Green's function and mean-field exchange-correlation potential, respectively, and $\Sigma_{\boldsymbol{k}}(\epsilon)$ is the self energy for the state $\boldsymbol{k}$.

While describing quasiparticle properties in many materials with high accuracy [20], the GW approximation is less reliable for satellite properties [12–14, 21]: for the spectral function of a core electron interacting with plasmons, GW predicts a single satellite instead of a satellite series with decreasing spectral weight and also greatly overestimates the binding energy of the satellite structures. The cumulant expansion [12–14, 17, 21, 22] of $G_{\boldsymbol{k}}(\epsilon)$ cures these deficiencies by including significant vertex corrections beyond GW: it provides the *exact* solution for a core electron interacting with plasmons [12]. In the cumulant approach, the Green's function for a hole is expressed as

$$G_{\boldsymbol{k}}(t) = i\Theta(-t)e^{-i\epsilon_{\boldsymbol{k}}t/\hbar + C_{\boldsymbol{k}}(t)}, \tag{2}$$

where $\epsilon_{\boldsymbol{k}}$ denotes the mean-field orbital energy and $C_{\boldsymbol{k}}(t)$ denotes the cumulant. This expression for the Green's function is obtained after the first iteration of the self-consistent solution of its equation of motion assuming a simple quasiparticle form for the starting guess [22].

The cumulant can be separated into a quasiparticle part $C^{qp}_{\boldsymbol{k}}(t)$ and a satellite part $C^{sat}_{\boldsymbol{k}}(t)$ given formally in terms of the self-energy by (for $t < 0$)

$$C^{qp}_{\boldsymbol{k}}(t) = -it\Sigma_{\boldsymbol{k}}(E_{\boldsymbol{k}})/\hbar + \frac{\partial\Sigma^h_{\boldsymbol{k}}(E_{\boldsymbol{k}})}{\partial\epsilon} \tag{3}$$

$$C^{sat}_{\boldsymbol{k}}(t) = \frac{1}{\pi}\int_{-\infty}^{\mu} d\epsilon \frac{\mathrm{Im}\Sigma_{\boldsymbol{k}}(\epsilon)}{(E_{\boldsymbol{k}} - \epsilon - i\eta)^2} e^{i(E_{\boldsymbol{k}}-\epsilon)t/\hbar}, \tag{4}$$

where μ denotes the chemical potential, η is a positive infinitesimal, $E_{\boldsymbol{k}} = \epsilon_{\boldsymbol{k}} + \Sigma_{\boldsymbol{k}}(E_{\boldsymbol{k}}) - V^{xc}_{\boldsymbol{k}}$ is the quasiparticle energy and $\Sigma^h_{\boldsymbol{k}}(\epsilon)$ is defined through the relation

$$\Sigma^h_{\boldsymbol{k}}(\epsilon) = \frac{1}{\pi}\int_{-\infty}^{\mu} d\epsilon' \frac{\mathrm{Im}\Sigma_{\boldsymbol{k}}(\epsilon')}{\epsilon' - \epsilon - i\eta}. \tag{5}$$

For a given level of approximation for Σ, the cumulant theory yields an improved Green's function through Eqs. (2-5). In the present study, Σ is obtained from GW theory [20, 23] which is known to describe quasiparticle properties in many materials accurately thus providing a good starting point for the cumulant theory.

Computational details.—We use Hartree theory as the starting mean-field theory, i.e. $V^{xc}_{\boldsymbol{k}} = 0$. The bare Coulomb interaction in an ideal 2DEG is $v(\boldsymbol{q}) = 2\pi e^2/|\boldsymbol{q}|$. We include the finite width ($w = 230$ Å[11]) of the electron gas of the experimental sample by multiplying $v(\boldsymbol{q})$ with a form factor [5]. To account for the screening by the surrounding dielectric environment we divide $v(\boldsymbol{q})$ by $\epsilon_\infty = 10.9$ corresponding to the $GaAs/Al_xGa_{1-x}As$ heterostructure of Dial et al. [11]. The metallic screening of the distant electrode (being at a distance $d = 245$ Å from the center of the quantum well [11]) is included by means of an image charge model [24]. We have investigated the sensitivity of the GW+C spectral functions on the environment screening, the electrode distance and the well width by varying the parameters by 10 percent and found the dependence to be quite weak [see Fig. 1(a)]. Screening processes within the 2DEG are described via its analytically known frequency-dependent polarizability function in the random-phase approximation[6]. We first calculate the imaginary part of the self energy and then carry out a Kramers-Kronig transformation to obtain the real part.

To improve the mean-field Green's function from Hartree theory, all mean-field energies are shifted by a constant Δ which is determined by requiring that $\hbar^2k_F^2/(2m^*) + \Delta$ ($m^* = 0.067m$ denoting the effective electron mass [11] with m being the bare electron mass and k_F the Fermi wave vector) equals the quasiparticle energy at k_F obtained by solving Dyson's equation. Finally, we used the self energy from the GW calculation to evaluate the spectral function in GW+C theory. We note that all results discussed below include the effects of finite quantum well widths and dielectric screening of the environment.

Results.—Figure 1(a) shows the spectral function for a 2DEG with $n = 5\times10^{10}/\mathrm{cm}^2$ at $k = 0$, i.e., at the bottom of the band, from GW and GW+C theories. Both spectral functions exhibit two peaks: one quasiparticle peak at a lower binding energy and a satellite peak at a higher binding energy. While the location of the quasiparticle peak is the same in both theories, the location and shape of the satellite peak is very different: GW theory gives a very sharp satellite peak at an energy of ~ -6.8 meV, while GW+C results in a much broader satellite structure with a weak peak at ~ -5.5 meV.

Unlike the three-dimensional electron gas where the plasmons are high-energy excitations with an energy scale of $\omega_{pl} = \sqrt{4\pi ne^2/m}$ with n denoting the electron volume density, the plasmons in the 2DEG have a dispersion of $\omega_{pl}(q) \approx \alpha(n)\sqrt{q}$ (in the long wavelength limit without metallic screening from the distant electrode) with $\alpha(n) = \sqrt{2\pi ne^2/(\epsilon_\infty m^*)}$. To understand the separation between the satellite and the quasiparticle peaks in Fig. 1(a), we expand the exponential factor in Eq. (2) into a power series in $C^{sat}_{\boldsymbol{k}}$, the satellite contribution to the cumulant function. The resulting spectral function is given by a quasiparticle contribution and an infinite sum of satellites, i.e. $A_{\boldsymbol{k}}(\epsilon) = A^{qp}_{\boldsymbol{k}}(\epsilon) + \sum_{n=1}^{\infty} A^{sat,n}_{\boldsymbol{k}}(\epsilon)$ with $A^{qp}_{\boldsymbol{k}}(\epsilon)$ being a Lorentzian centered at $E_{\boldsymbol{k}}$ and $A^{sat,1}_{\boldsymbol{k}}(\epsilon) = \int d\epsilon' C^{sat}_{\boldsymbol{k}}(\epsilon')A^{qp}_{\boldsymbol{k}}(\epsilon - \epsilon') \approx Z_{\boldsymbol{k}}C^{sat}_{\boldsymbol{k}}(\epsilon - E_{\boldsymbol{k}})$ with $Z_{\boldsymbol{k}}$ denoting the renormalization factor. According to Eq. (4), $C^{sat}_{\boldsymbol{k}}(\epsilon - E_{\boldsymbol{k}})$ is proportional to the imaginary part of the self energy which has a van Hove singularity when the group velocity of the holes equals the plasmon

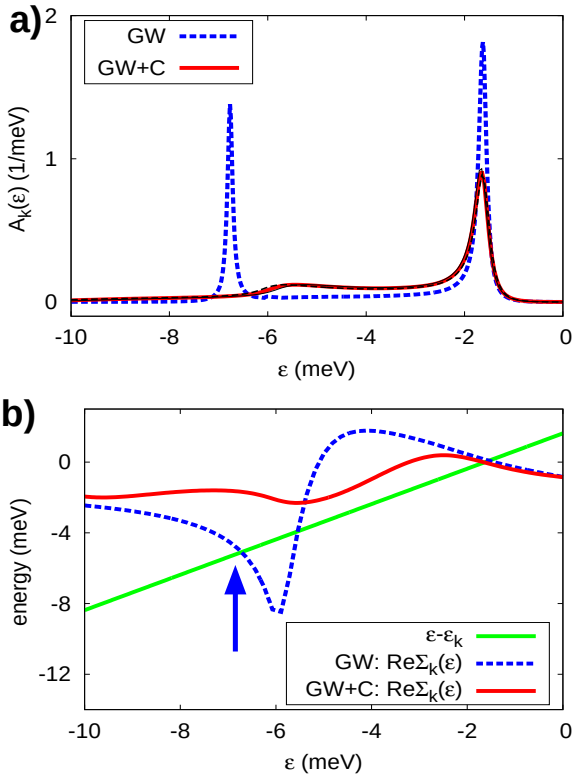

FIG. 1: (a): Spectral functions at $k = 0$ for $n = 5 \times 10^{10}/\mathrm{cm}^2$ from GW and GW+C theories. Also shown are the GW+C spectral functions obtained by increasing (solid black line) and decreasing (dashed black line) the environment dielectric constant, the electrode distance and the well width by 10 percent. (b): Real parts of the self energies from GW and GW+C theories. The arrow indicates the plasmaron solution in GW theory. All energies are measured with respect to the Fermi energy.

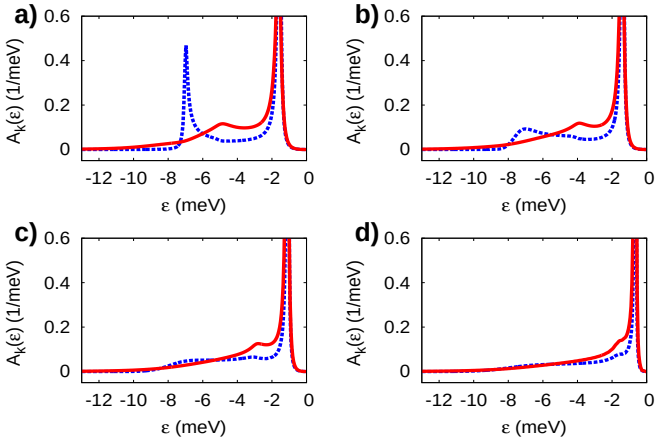

FIG. 2: Spectral functions at (a) $k = 0.2\ k_F$, (b) $k = 0.4\ k_F$, (c) $k = 0.6\ k_F$ and (d) $k = 0.8\ k_F$ for $n = 5 \times 10^{10}/\mathrm{cm}^2$ from GW+C (solid red curves) and GW (dashed blue curves) theories. All energies are measured with respect to the Fermi energy.

group velocity. For $k = 0$, this argument predicts a separation of $\Delta E = [\hbar^2 m^* \alpha(n)^4/2]^{1/3} \approx 4.6$ meV between the quasiparticle peak and the satellite. This is somewhat larger, but agrees reasonably well with the separation $\Delta E = 3.8$ meV found in Fig. 1(a) from the full GW+C theory.

The discrepancy between GW and GW+C theory for the shape and location of the satellite peak can be traced back to a spurious pole of the Green's function in GW theory. Figure 1(b) shows the graphical solution of Dyson's equation for GW and GW+C theory. For GW+C, we computed the vertex-corrected self energy via $\Sigma_{\boldsymbol{k}}(\epsilon) = \epsilon - \epsilon_{\boldsymbol{k}} - G^{-1}_{\boldsymbol{k}}(\epsilon)$ with $G_{\boldsymbol{k}}(\epsilon)$ obtained from Eq. (2). The sharp satellite peak in the GW spectral function results from an additional solution of Dyson's equation. Such an additional solution on the real frequency axis was first found in the three-dimensional electron gas by Lundqvist who introduced the term *plasmaron* describing a hole resonantly bound to plasmons[18]. No such solution is found in the GW+C theory indicating the disappearance of the plasmaron excitation when higher-order electron-electron interactions are included. The origin of the spurious plasmaron solution is thus a failure of GW theory, which replaces all satellites peaks by a *single, effective* satellite at an artificially high binding energy [12]. Physically, the satellites in the GW+C theory correspond to many-body states consisting of weakly interacting hole-plasmon pairs.

Figures 2 and 3 show results for spectral functions at larger wave vectors: Fig. 2(a) shows that, also at nonzero but small wave vectors, GW theory gives a strong plasmaron satellite. Fig. 3 shows that this GW plasmaron branch disperses towards higher binding energies with increasing k and then disappears at $k \approx 0.25\ k_F$. Interestingly, there is an additional satellite branch in GW theory: it is much weaker than the plasmaron branch and merges with the quasiparticle branch at k_F.

Figure 3(b) shows that no plasmaron branch is found in GW+C theory. We also find a satellite branch which merges with the quasiparticles at k_F and is somewhat stronger than the corresponding weak feature in GW. Figure 2(d) shows that near k_F the spectral functions in GW and GW+C are more similar than at small k.

Figures 4(a)-(c) show the resulting DOS from GW and GW+C theories for different electron densities. The sharp increase at low binding energies [for example, in Fig. 4(a) at ~ -2 meV] is due to the quasiparticle contribution to the DOS. Without electron-electron interactions the DOS is a step function of height $g_0 = m^*/(\pi\hbar^2)$ with a sharp onset at $-\hbar^2 k_F^2/(2m^*)$. The feature at higher binding energies is caused by plasmon satellites and is very different in GW and GW+C theories. GW theory results in a plateau-like feature [between ~ -7 and ~ -2 meV in Fig. 4(a)] followed by a peak (arising from plasmaron excitations) at -7 meV and a decaying

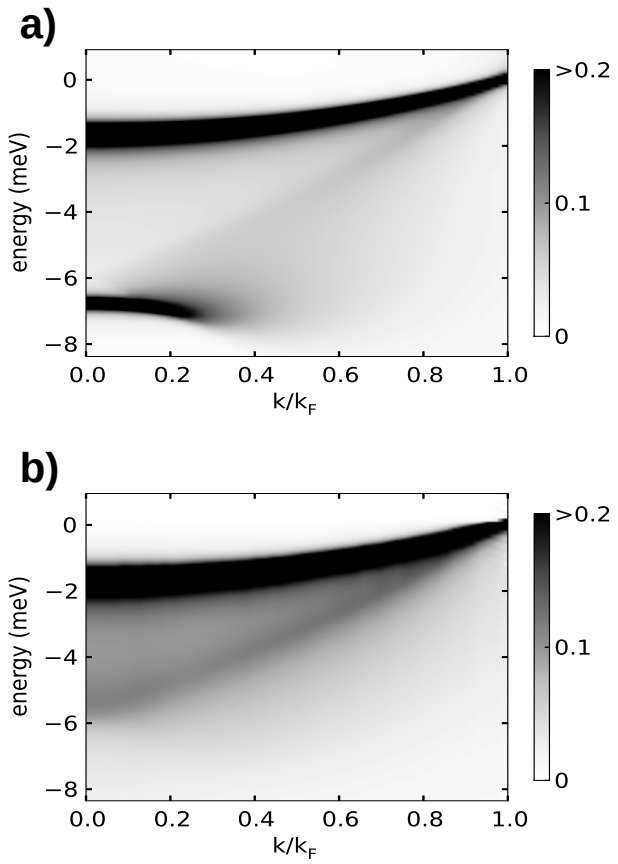

FIG. 3: Spectral functions $A_{k}(\epsilon)$ (in units of 1/meV) of a two-dimensional electron gas with $n = 5 \times 10^{10}/\mathrm{cm}^2$ from (a) GW and (b) GW+C theories. All energies are measured with respect to the Fermi level.

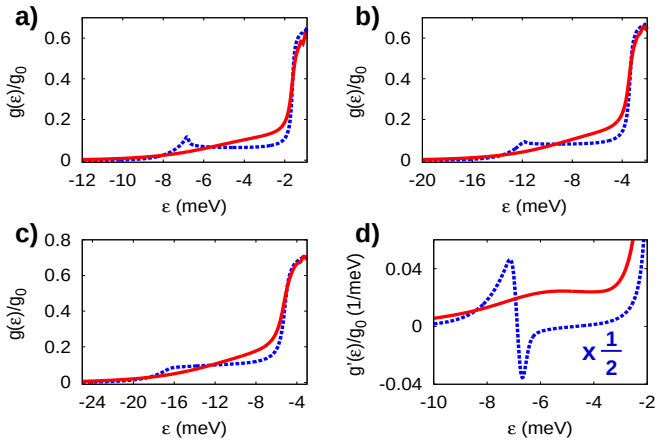

FIG. 4: DOS of a 2DEG with (a) $n = 5 \times 10^{10}/\mathrm{cm}^2$, (b) $n = 10 \times 10^{10}/\mathrm{cm}^2$ and (c) $n = 15 \times 10^{10}/\mathrm{cm}^2$ from GW (dashed blue curves) and GW+C (solid red curves) theories. (d): $g'(\epsilon) = dg(\epsilon)/d\epsilon$ for $n = 5 \times 10^{10}/\mathrm{cm}^2$. We have divided $dg/d\epsilon$ from GW by a factor of 2 to simplify the comparison with the GW+C result. $g_0 = m^*/(\pi\hbar^2)$ denotes the value of the DOS neglecting electron-electron interactions. All energies are measured with respect to the Fermi energy.

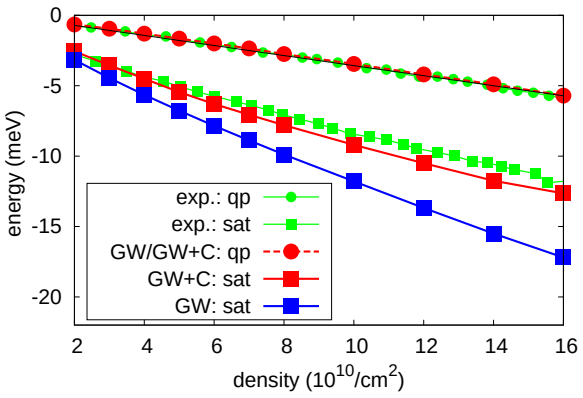

FIG. 5: Quasiparticle (qp) and satellite (sat) band edge positions from GW theory, GW+C theory and experiment [11]. The dashed black line shows the quasiparticle band edge position from Hartree theory.

tail. In the GW+C theory we do not observe such a plateau in the DOS, but instead a tail which starts at the edge of the quasiparticle feature and decays slowly with increasing binding energy.

Direct comparisons of the computed DOS and experimental dI/dV curves are difficult due to complicated matrix element effects [9]. To analyze the main features in the DOS, we follow the procedure of Ref.[11] and compute the derivative of the DOS which — assuming the electrode DOS and the matrix element are slowly varying functions of ϵ — is proportional to d^2I/dV^2 [11]. Fig. 4(d) shows that in GW theory the plasmaron peak at the edge of the satellite structure causes a characteristic feature in $dg/d\epsilon$: a sharp negative dip followed by a positive peak as a function of increasing binding energy. Instead, we find a broad peak in $dg/d\epsilon$ from GW+C theory.

Figure 5 shows the peak locations in $dg/d\epsilon$ for different electron densities and compares the results of GW and GW+C calculations with the experimental data of Dial and coworkers. For the feature corresponding to the onset of the quasiparticle structure at low binding energies, both GW and GW+C theories agree very well with experiment. For the second feature at higher binding energy arising from the satellite structure in the DOS, GW+C theory agrees much better with experiment than GW theory. This indicates that the plasmaron solutions in GW theory are indeed not physical. We attribute the remaining small difference between GW+C theory and experiment to interactions with phonons. The longitudinal optical phonon mode of gallium arsenide couples weakly to the electrons in the 2DEG. Das Sarma and coworkers have shown that this results in a small decrease of the satellite band edge binding energy in GW theory and we expect that phonons will have a similar effect in GW+C theory [5].

In conclusion, we have carried out GW+C calculations for the two-dimensional electron gas in GaAs quantum wells at various densities and found good agreement with the experimental findings of Dial and coworkers [11]. Our results for the satellite structures disagree qualitatively and quantitatively with calculations based on the GW approximation only to the electron self energy. In particular, we do not find a plasmaron excitation in GW+C theory.

J.L. acknowledges valuable discussions with Oliver Dial and Raymond Ashoori. S. G. L. acknowledges support by a Simons Foundation Fellowship in Theoretical Physics. This work was supported by NSF Grant No. DMR10-1006184 (numerical simulations of the two-dimensional electron gas) and by the Theory Program at the Lawrence Berkeley National Laboratory funded by the Director, Office of Science, Office of Basic Energy Sciences, Division of Materials Sciences and Engineering Division, US Department of Energy under Contract No. DE-AC02-05CH11231 (methods and software development of electron correlation effects).

[1] K. von Klitzing, G. Dorda, and M. Pepper, Phys. Rev. Lett. **45**, 454 (1980).
[2] D. C. Tsui, H. L. Stormer, and A. C. Gossard, Phys. Rev. Lett. **48**, 1559 (1982).
[3] A. Ohtomo and H. Y. Hwang, Nature **427**, 423 (2004).
[4] C. H. Ahn, J.-M. Triscone, and J. Mannhart, Nature **424**, 1015 (2003).
[5] E. H. Hwang and S. D. Sarma, Phys. Rev. B **77**, 081412(R) (2008).
[6] T. Ando, A. B. Fowler, and F. Stern, Rev. Mod. Phys. **54**, 437 (1982).
[7] B. Tanatar and D. M. Ceperley, Phys. Rev. B **39**, 5005 (1989).
[8] N. D. Drummond and R. J. Needs, Phys. Rev. Lett. **102**, 126402 (2009).
[9] O. E. Dial, R. C. Ashoori, L. N. Pfeiffer, and K. W. West, Nature (London) **448**, 176 (2007).
[10] O. E. Dial, R. C. Ashoori, L. N. Pfeiffer, and K. W. West, Nature (London) **464**, 566 (2010).
[11] O. E. Dial, R. C. Ashoori, L. N. Pfeiffer, and K. W. West, Phys. Rev. B **85**, 081306(R) (2012).
[12] D. C. Langreth, Phys. Rev. B **1**, 471 (1970).
[13] M. Guzzo, G. Lani, F. Sottile, P. Romaniello, M. Gatti, J. J. Kas, J. J. Rehr, M. G. Silly, F. Sirotti, and L. Reining, Phys. Rev. Lett. **107**, 166401 (2011).
[14] J. Lischner, D. Vigil-Fowler, and S. G. Louie, Phys. Rev. Lett. **110**, 146801 (2013).
[15] J. Lischner, D. Vigil-Fowler, and S. G. Louie, ? **?**, ? (2013).
[16] A. Bostwick, F. Speck, T. Seyller, K. Horn, M. Polini, R. Asgari, A. H. MacDonald, and E. Rotenberg, Science **328**, 999 (2010).
[17] L. Hedin, Physica Scripta **21**, 477 (1980).
[18] B. I. Lundqvist, Phys. kondens. Materie **6**, 193 (1967).
[19] E. Kaxiras, *Atomic and Electronic Structure of Solids* (Cambridge, 2003).
[20] M. S. Hybertsen and S. G. Louie, Phys. Rev. B **34**, 5390 (1986).
[21] F. Aryasetiawan, L. Hedin, and K. Karlsson, Phys. Rev. Lett. **77**, 2268 (1996).
[22] C.-O. Almbladh and L. Hedin, *Handbook of Synchroton Radiation*, vol. 1 (E. E. Koch (North-Holland, Amsterdam), 1983).
[23] L. Hedin and S. Lundqvist, Solid State Physics **23**, 1 (1970).
[24] J. B. Neaton, M. S. Hybertsen, and S. G. Louie, Phys. Rev. Lett. **97**, 216405 (2006).